

Ultrafast magnetization dynamics in half-metallic Co₂FeAl Heusler alloy

R. S. Malik,¹ E. K. Delczeg-Czirjak,¹ D. Thonig,² R. Knut,¹ I. Vaskivskyi,¹
R. Gupta,³ S. Jana,¹ R. Stefanuik,¹ Y. O. Kvashnin,¹ S. Husain,³ A.
Kumar,³ P. Svedlindh,³ J. Söderström,¹ O. Eriksson,^{1,2} and O. Karis¹

¹*Department of Physics and Astronomy,
Uppsala University, Box 516, SE-75120, Uppsala, Sweden*

²*School of Science and Technology,
Örebro University, SE-70182 Örebro, Sweden*

³*Department of Materials Science and Engineering,
Uppsala University, Box 534, SE-75121, Uppsala, Sweden*

Abstract

We report on optically induced, ultrafast magnetization dynamics in the Heusler alloy Co₂FeAl, probed by time-resolved magneto-optical Kerr effect. Experimental results are compared to results from electronic structure theory and atomistic spin-dynamics simulations. Experimentally, we find that the demagnetization time (τ_M) in films of Co₂FeAl is almost independent of varying structural order, and that it is similar to that in elemental 3d ferromagnets. In contrast, the slower process of magnetization recovery, specified by τ_R , is found to occur on picosecond time scales, and is demonstrated to correlate strongly with the Gilbert damping parameter (α). Our results show that Co₂FeAl is unique, in that it is the first material that clearly demonstrates the importance of the damping parameter in the remagnetization process. Based on these results we argue that for Co₂FeAl the remagnetization process is dominated by magnon dynamics, something which might have general applicability.

Studies of ultrafast demagnetization was pioneered by Beaurepaire *et al.*[1], who demonstrated that the optical excitation of a ferromagnetic material - using a short pulsed laser could quench the magnetic moment on sub-picosecond timescales. The exact underlying microscopic mechanisms responsible for the transfer of angular momentum have been strongly debated for more than 20 years [2–4]. Ultrafast laser-induced demagnetization has now become an intense field of research not only from fundamental point of view but also from a technological aspect, due to an appealing possibility to further push the limits of operation of information storage and data processing devices [5]. Both experiment [4–15] and theory [16–23] report that all of the 3d ferromagnets (Fe, Ni and Co) and their alloys, show characteristic demagnetization times in the sub-picosecond range, while 4f metals exhibit a complicated two-step demagnetization up to several picoseconds after the excitation pulse [4, 24].

In this work, we have made element specific investigations of the ultrafast magnetization dynamics of a half-metallic Heusler alloy. This class of alloys has been investigated intensively, especially concerning the magnetic properties, ever since the discovery in 1903, when Heusler *et al.* reported that alloys like Cu_2MnAl exhibit ferromagnetic properties, even though none of its constituent elements was in itself ferromagnetic [25]. The ferromagnetic properties were found to be related to the chemical ordering [26]. One of the key features of several Heusler alloys is their unique electronic structure, where the majority spin band-structure has a metallic character while the minority spin band is semiconducting with a band gap. Such materials are also referred to as half-metallic ferromagnets (HMFs) and were initially predicted by de Groot *et al.* [27], based on electronic structure theory. Half-metals ideally exhibit 100% spin-polarization at the Fermi level. This exclusive property makes them candidates to be incorporated in spintronic devices, e.g. spin filters, tunnel junctions and giant magneto-resistance (GMR) devices [28–31]. One of the advantages of Heusler alloys with respect to other half-metallic system, like CrO_2 and Fe_3O_4 , are their relatively high Curie temperature (T_c) and low coercivity (H_c) [32, 33]. Heusler alloys are also appealing for spintronic applications due to the low Gilbert damping, which allows for a long magnon diffusion length [34–39]. It has been shown that the low value of the Gilbert damping constant is related with the half-metallicity [37, 38]. The origin of the band gap and the mechanism of half-metallicity in these materials have been studied by using first principle electronic structure calculations [40–43]. The half-metallic property is furthermore

known to be very sensitive to structural disorder [41–45]. From a fundamental point of view, it is intriguing to ask, how the band gap in the minority spin channel effects the ultrafast magnetization dynamics of Heusler alloys [46, 47]. It has already been reported that some of the half-metals like CrO_2 and Fe_3O_4 exhibit very slow dynamics, involving time-scales of hundreds of picoseconds, [46, 47] while several Co-based Heusler alloys show a much faster demagnetization, similar to the time-scales of the elemental 3d-ferromagnets [48–50]. The faster dynamics of these Heuslers has been discussed in Ref.[46] to be due to the fact that the band gap in the minority spin channel is typically around $0.3 - 0.5$ eV, which is smaller than the photon energy (1.5 eV) of the exciting laser. It is also smaller than the band gap of CrO_2 and Fe_3O_4 . Importantly, the Heusler alloys offer the possibility to study magnetization dynamics, as a function of structural order, since they normally can be prepared to have a fully ordered $L2_1$ phase, a partially ordered $B2$ phase, and a completely disordered $A2$ phase. The structural relationships of these phases are described in the Supplemental Material (SM) [51].

We have here studied the optically induced, ultrafast magnetization dynamics of Co_2FeAl (CFA) films, using time-resolved magneto-optical Kerr effect (TR-MOKE) as described in Ref. [52]. By control of the growth temperature, CFA alloy forms with varying degree of structural order, in a continuous way between the $A2$ and $B2$ phases, as well as between the $B2$ and $L2_1$ phases [53, 54]. We present data from four CFA samples, grown at 300 K, 573 K, 673 K, and 773 K respectively. We henceforth denote each sample by its growth temperature as a subscript, e.g. $\text{CFA}_{300\text{K}}$. As evidenced by X-ray diffraction, the sample grown at 300 K is found to exhibit the $A2$ phase, while the samples grown at 573 K and 673 K predominantly exhibit the $B2$ phase. The sample grown at 773 K is found to exhibit a pure $B2$ phase [54]. The value of the Gilbert damping α is found to monotonously decrease with annealing temperature and is thus lowest for the sample grown at 773 K [55].

Calculations based on density functional theory (DFT) of the magnetic moment, Heisenberg exchange interaction and the Gilbert damping parameter are described in detail in (SM) [51]. These parameters were used in a multiscale approach to perform atomistic magnetization dynamics simulations, described in Sec.S1 of (SM) [51]. Here we employed the two temperature model (2TM) for the temperature profile of the spin-system. In the 2TM, the spin temperature increases due to the coupling to the hot-electron bath, that is excited by the external laser pulse. In the simulations we used a peak temperature in the 2TM of

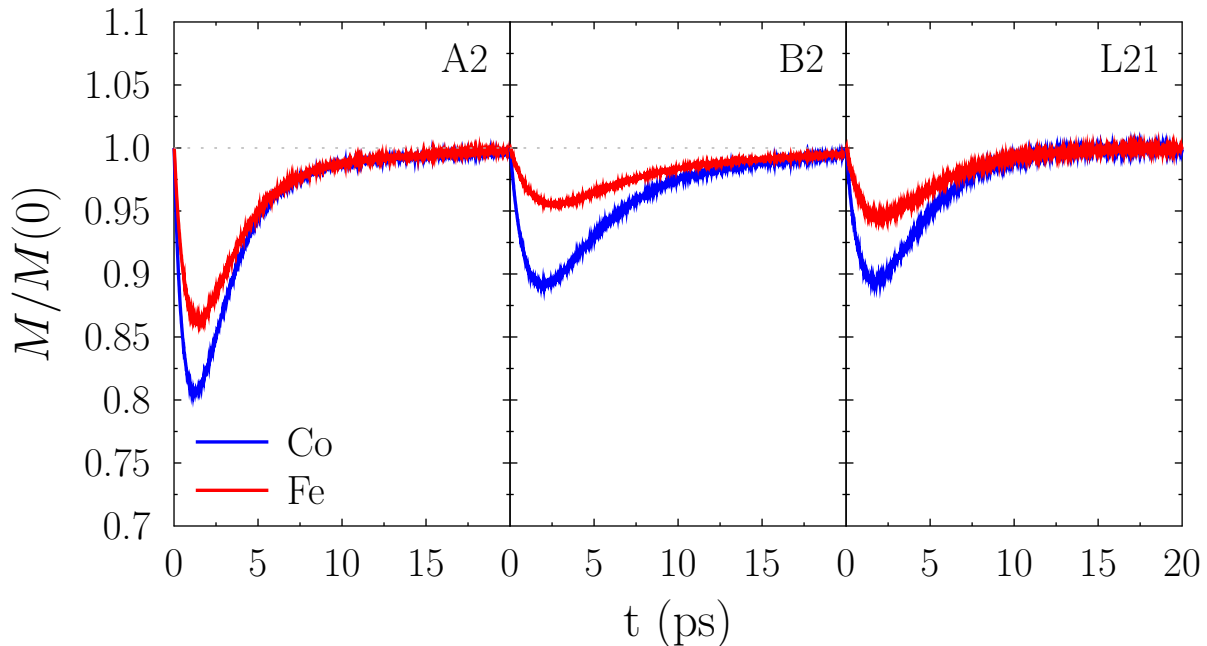


FIG. 1. (Color online) Simulations of ultrafast dynamics of Co_2FeAl in the different structural phases $A2$ (left panel), $B2$ (central panel), and $L2_1$ (right panel). The demagnetization is shown element resolved (blue line - Co, red line - Fe). The peak temperature is 1200 K. The dotted line indicates the equilibrium magnetization at $T = 300$ K.

1200 K. A full description of the 2TM and the details of all spin-dynamics simulations are described in Sec.S2 of SM [51].

The results of the simulations are shown in Fig. 1, for the $A2$, $B2$ and $L2_1$ phases. It can be seen that the different phases react differently to the external stimulus. In general, this model provides a dynamics that is controlled by *i*) the temperature of the spin-subsystem, *ii*) the strength of the magnetic exchange interaction and *iii*) the dissipation of angular momentum and energy during the relaxation of the atomic magnetic moments (Gilbert damping) [56]. Before continuing the discussion, we note that the average magnetization, M , of element X is calculated as $M^X = \sum_i c_i^X M_i^X / 4 \sum_i c_i^X$, where c_i^X is the concentration of the particular element X in the particular phase and i runs over the four nonequivalent sites of the unit cell. After the material demagnetizes, the spin temperature eventually drops and the average magnetization returns to its initial value after 10 – 20 ps (cf. Fig. 1).

To estimate the time constants of the demagnetization τ_M and remagnetization (τ_R)

processes, in an element-specific way, we fit both the theoretical and experimental transient magnetizations by a double exponential function [57]. We show results of τ_M and τ_R in Fig. 2 for the $A2$ and $B2$ phase, as well as for alloys with intermediate degree of disorder (described in Sec.S2 of SM [51]).

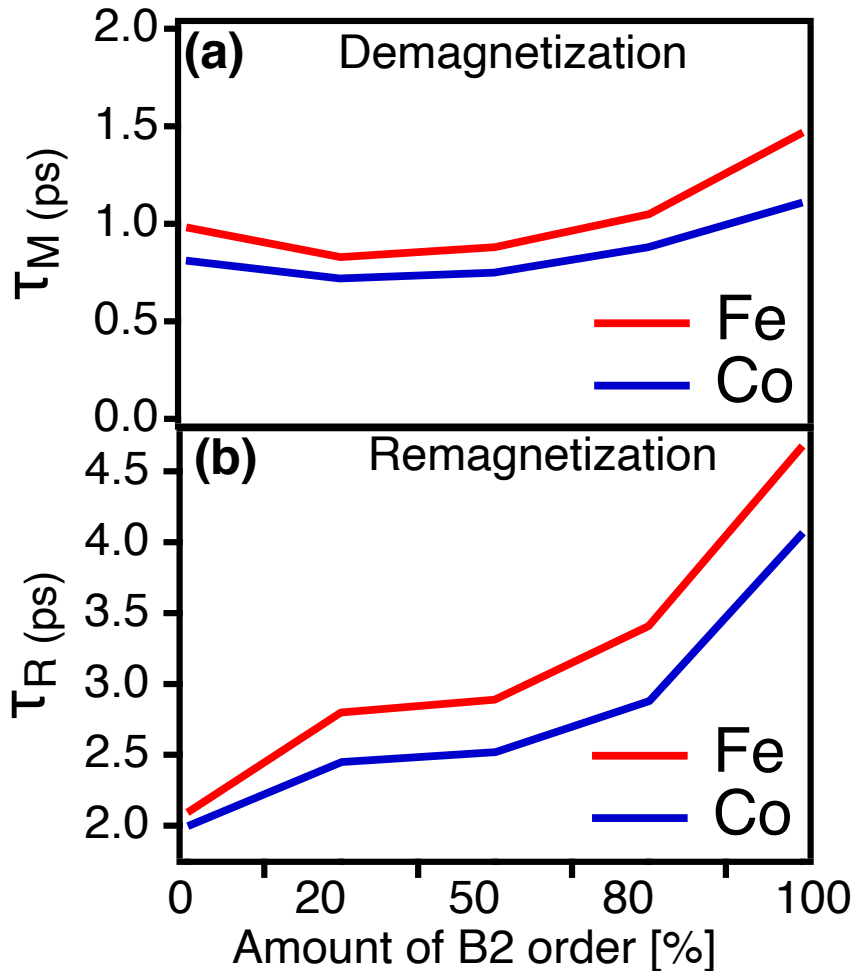


FIG. 2. (Color online) Element resolved relaxation times of Co_2FeAl , from simulations of alloys with varying amounts of $A2 \rightarrow B2$ phase. 0 corresponds to pure $A2$ phase while 100 corresponds to pure $B2$ phase. Panel (a) shows the demagnetization time and panel (b) shows the remagnetization time. Both time constants are obtained from fitting the time trajectory of $M^X(t)$ by a double-exponential function (see text).

The theoretical demagnetization time is seen from Fig. 2 to typically be around 1 ps, whereas the remagnetization time is 2 – 5 ps. Going from the $A2$ to the $B2$ alloy, both times increase, albeit the simulations show a stronger increase of the remagnetization time

as function of alloy composition. We also note that the relevant time scale is somewhat larger for Fe than for Co, and the ratio between them, τ_{Fe}/τ_{Co} , grows when going from $A2$ to $B2$ phase.

Figures 3 (a-d) shows the measured magnetization dynamics of CFA films that were grown at different temperatures (see SM, Sec.S3 for thin films synthesis, and Sec.S4 for details on the experimental measurements [51]). The inset shows the observed magnetization dynamics up to ~ 1 ps. For all samples, the data for Fe (red) and Co (blue) show similar demagnetization dynamics in the first few hundred femtoseconds, whereupon differences in the magnetization dynamics become visible, especially on the picosecond timescale.

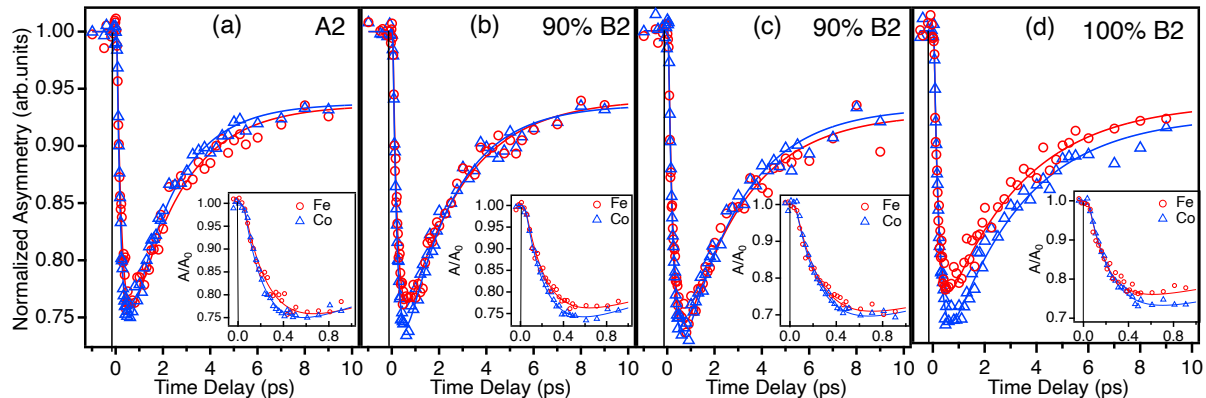


FIG. 3. Measured element-specific Fe (red) and Co (blue) magnetization dynamics of Co_2FeAl . Samples are denoted by the growth temperature in each case. The red and blue lines correspond to fitted data (see text). (a) 300 K (100% A_2 phase), (b) 573 K (90% B_2 phase), (c) 673 K (90% B_2 phase), and (d) 773 K (100% B_2 phase). The insets show the demagnetization dynamics up to ~ 1 ps. All of the measurements were performed with similar pump-fluence (for details, see Sec.S4 of SM).

Figure 4 (a-b) shows the measured values of the demagnetization and remagnetization time constants, for the four different growth temperatures, representing different degree of disorder in Co_2FeAl , along the alloy path $A_2 \rightarrow B_2$. It may be seen that the τ_M for Fe and Co is the same within the error bars for all four samples, regardless of the degree of structural ordering (Fig. 4a). It may also be noted that the measured τ_M for CFA is similar to that of 3d transition metals [48, 49] and very much shorter than that of CrO_2 or Fe_3O_4 .

Demagnetization times that are independent on degree of structural ordering is interest-

ing, since it can be expected that the presence of structural disorder in Heusler alloys ought to result in a lower degree of spin polarization of the electronic states (i.e. an increased density of states (DOS) at the Fermi level in the minority band). This is expected to enhance spin-flip scattering, with an accompanying speed-up of the demagnetization dynamics [46, 47]. The electronic structure calculation of CFA also shows that the DOS at the Fermi level varies with different structural phases (analyzed in the Sec.S1 of SM [51]). The $A2$ phase has a large number of states at the Fermi level, while the $L2_1$ phase, and to some extent the $B2$ phase, has a low amount [54]. Despite these differences in the electronic structure, the measured demagnetization dynamics shown in Fig. 4(a) is essentially independent on degree of structural ordering.

On longer time-scales, there is a significant effect of structural ordering on the observed magnetization dynamics, which becomes particularly relevant for the remagnetization process. As seen in Fig. 4b, there is a monotonous increase of remagnetization time, τ_R , with increasing growth temperature and hence the degree of ordering along the $A2 \rightarrow B2$ path. The sample grown at 300 K with $A2$ phase, exhibits the fastest remagnetization dynamics (τ_R). With increasing growth temperature and corresponding increase in the structural ordering along the $A2 \rightarrow B2$ path, a distinct trend of increasingly slower remagnetization dynamics is observed.

The most conspicuous behaviour of the measured magnetization dynamics, and its dependence on the degree of ordering, concerns the remagnetization time (Fig. 4b). The time-scale of the remagnetization process is sufficiently long to allow for an interpretation based on atomistic spin-dynamics. Two materials specific parameters should be the most relevant to control this dynamics; the exchange interaction, as revealed by the local Weiss field, and the damping parameter. In the Sec.S2 of SM [51], we report on the calculated Weiss fields and damping parameters. It is clear from these results that the trend in the experimental data shown in Fig. 4b, can not be understood from the Weiss field alone, whereas an explanation based on the damping is more likely. In order to illustrate this, we show in Fig. 5 the inverse of the measured remagnetization time compared to the theoretically calculated damping and experimental measured damping through ferromagnetic resonance (FMR) (described in Sec.S6 of SM)[51]. The figure shows that the damping is large in the completely disordered $A2$ phase and for a large range of structural orderings, which comes out from both theory and experiment. The figure also demonstrates that the inverse of the measured

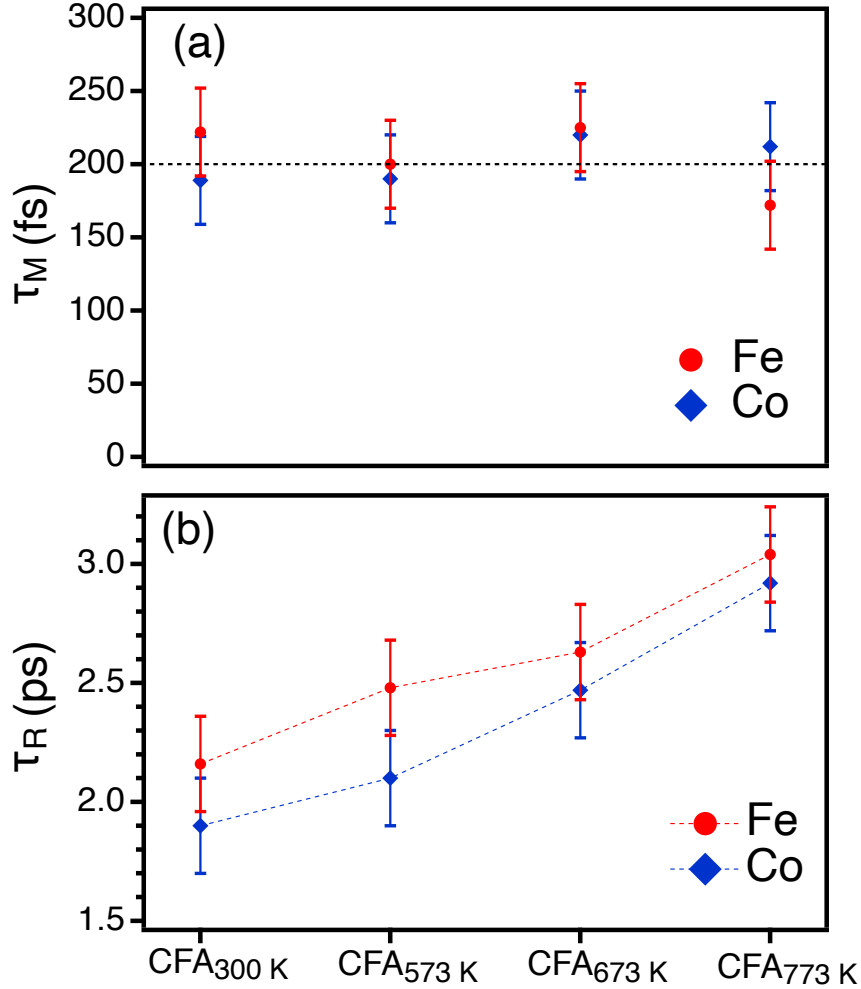


FIG. 4. Measured magnetization times for the investigated Co_2FeAl alloys. In (a) the demagnetization time, τ_M , is shown and in (b) the remagnetization time, τ_R , is plotted.

remagnetization time scales very well with both the calculated damping and experimentally measured damping. According to the figure, a large damping parameter corresponds to faster remagnetization dynamics in the measurements.

Co_2FeAl is, to the best of our knowledge, the first system where experimental observations and theory point to the importance of damping in the process of ultrafast magnetization dynamics. We note that this primarily is relevant for the remagnetization process; the initial part of the magnetization dynamics (first few hundred fs) is distinctly different. In the demagnetization we observe a similar behaviour for Fe and Co in all samples, and an insensitivity of the demagnetization times in relation to structural ordering. Also, the

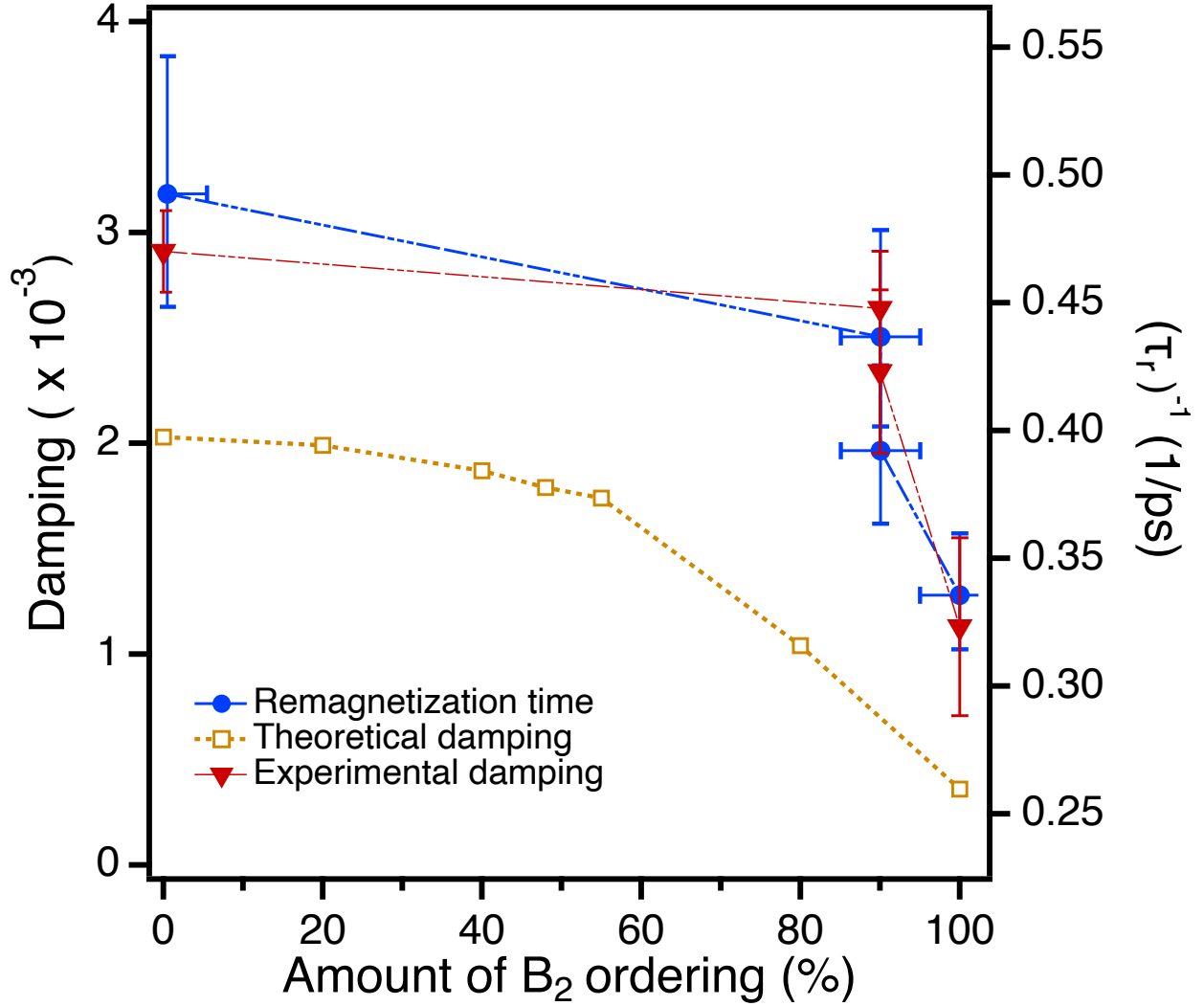


FIG. 5. The relationship of inverse of the measured remagnetization time (right y-axis) and theoretically calculated and experimentally measured Gilbert damping (left y-axis) in Co_2FeAl for varying amount of B2 order along the $A2 \rightarrow B2$ path, i.e. 0 corresponds to pure A2 phase while 100 corresponds to pure B2 phase.

measured and theoretical demagnetization times evaluated from atomistic spin-dynamics simulations, do not agree. Other mechanisms, of electronic origin, most likely play role in this temporal regime.

The remagnetization process of Co_2FeAl alloys with varying degree of structural order, highlights clearly the importance of the Gilbert damping and that magnon dynamics domi-

nates the magnetization at ps time-scales. The relevance of the Gilbert damping parameter for ps dynamics is natural, since this controls angular momentum (and energy) transfer to the surrounding. What is surprising with Co₂FeAl is the fact that other interactions (e.g. the Weiss field) show such a weak dependence on the amount of structural disorder. This is fortuitous, since it allows to identify the importance of the Gilbert damping. A picture emerges from the results presented here, that the magnetization dynamics in general have two regimes; one which is primarily governed by electronic processes, and is mainly active in the first few hundred fs (τ_M), and a second regime where it is primarily magnons that govern the remagnetization dynamics (τ_R).

We acknowledge support from the Swedish Research Council (VR, contracts 2019-03666,201703799, 2016-04524 and 2013-08316), the Swedish Foundation for Strategic Research, project SSF Magnetic materials for green energy technology under Grant No. EM16-0039, the Knut and Alice Wallenberg foundation, STandUP and eSSENCE, for financial support. The Swedish National Infrastructure for Computing (SNIC) is acknowledged for computational resources.

-
- [1] E. Beaurepaire, J.-C. Merle, A. Daunois, and J.-Y. Bigot, Phys. Rev. Lett. **76**, 4250 (1996).
 - [2] A. Scholl, L. Baumgarten, R. Jacquemin, and W. Eberhardt, Phys. Rev. Lett. **79**, 5146 (1997).
 - [3] B. Koopmans, J. J. M. Ruigrok, F. D. DallaLonga, and W. J. M. de Jonge, Phys. Rev. Lett. **95**, 267207 (2005).
 - [4] B. Koopmans, G. Malinowski, F. Dalla Longa, D. Steiauf, M. Fähnle, T. Roth, M. Cinchetti, and M. Aeschlimann, Nat. Mater. **9**, 259 (2010).
 - [5] A. Kirilyuk, A. V. Kimel, and T. Rasing, Rev. Mod. Phys. **82**, 2731 (2010).
 - [6] M. Cinchetti, M. Sánchez Albaneda, D. Hoffmann, T. Roth, J.-P. Wüstenberg, M. Krauß, O. Andreyev, H. C. Schneider, M. Bauer, and M. Aeschlimann, Phys. Rev. Lett. **97**, 177201 (2006).
 - [7] C. Stamm, T. Kachel, N. Pontius, R. Mitzner, T. Quast, K. Holldack, S. Khan, C. Lupulescu, E. Aziz, M. Wietstruk, *et al.*, Nat. Mater. **6**, 740 (2007).
 - [8] F. Dalla Longa, J. T. Kohlhepp, W. J. M. de Jonge, and B. Koopmans, Phys. Rev. B **75**, 224431 (2007).

- [9] J. Walowski, G. Müller, M. Djordjevic, M. Münzenberg, M. Kläui, C. A. F. Vaz, and J. A. C. Bland, *Phys. Rev. Lett.* **101**, 237401 (2008).
- [10] E. Carpene, E. Mancini, C. Dallera, M. Brenna, E. Puppini, and S. De Silvestri, *Phys. Rev. B* **78**, 174422 (2008).
- [11] T. Roth, A. J. Schellekens, S. Alebrand, O. Schmitt, D. Steil, B. Koopmans, M. Cinchetti, and M. Aeschlimann, *Phys. Rev. X* **2**, 021006 (2012).
- [12] S. Mathias, C. La-O-Vorakiat, P. Grychtol, P. Granitzka, E. Turgut, J. M. Shaw, R. Adam, H. T. Nembach, M. E. Siemens, S. Eich, C. M. Schneider, T. J. Silva, M. Aeschlimann, M. M. Murnane, and H. C. Kapteyn, *Proc. Natl. Acad. Sci. USA*. **109**, 4792 (2012).
- [13] D. Rudolf, C. La-O-Vorakiat, M. Battiato, R. Adam, J. M. Shaw, E. Turgut, P. Maldonado, S. Mathias, P. Grychtol, H. T. Nembach, T. J. Silva, M. Aeschlimann, H. C. Kapteyn, M. M. Murnane, C. M. Schneider, and P. M. Oppeneer, *Nat. Commun.* **3**, 1037 (2012).
- [14] A. Eschenlohr, M. Battiato, P. Maldonado, N. Pontius, T. Kachel, K. Holldack, R. Mitzner, A. Föhlisch, P. M. Oppeneer, and C. Stamm, *Nat. Mater.* **12**, 332 (2013).
- [15] E. Turgut, C. La-o vorakiat, J. M. Shaw, P. Grychtol, H. T. Nembach, D. Rudolf, R. Adam, M. Aeschlimann, C. M. Schneider, T. J. Silva, M. M. Murnane, H. C. Kapteyn, and S. Mathias, *Phys. Rev. Lett.* **110**, 197201 (2013).
- [16] G. P. Zhang and W. Hübner, *Phys. Rev. Lett.* **85**, 3025 (2000).
- [17] B. Koopmans, H. Kicken, M. Van Kampen, and W. De Jonge, *J. Magn. Magn. Mater.* **286**, 271 (2005).
- [18] M. Krauß, T. Roth, S. Alebrand, D. Steil, M. Cinchetti, M. Aeschlimann, and H. C. Schneider, *Phys. Rev. B* **80**, 180407 (2009).
- [19] D. Steiauf and M. Föhnle, *Phys. Rev. B* **79**, 140401 (2009).
- [20] J.-Y. Bigot, M. Vomir, and E. Beaurepaire, *Nat. Phys.* **5**, 515 (2009).
- [21] M. Battiato, K. Carva, and P. M. Oppeneer, *Phys. Rev. Lett.* **105**, 027203 (2010).
- [22] S. Essert and H. C. Schneider, *Phys. Rev. B* **84**, 224405 (2011).
- [23] U. Atxitia and O. Chubykalo-Fesenko, *Phys. Rev. B* **84**, 144414 (2011).
- [24] I. Radu, C. Stamm, A. Eschenlohr, F. Radu, R. Abrudan, K. Vahaplar, T. Kachel, N. Pontius, R. Mitzner, K. Holldack, A. Föhlisch, T. A. Ostler, J. H. Mentink, R. F. L. Evans, R. W. Chantrell, A. Tsukamoto, A. Itoh, A. Kirilyuk, A. V. Kimel, and T. Rasing, *SPIN* **05**, 1550004 (2015).

- [25] F. Heusler, W. Starck, and E. Haupt, *Verh. Dtsch. Phys. Ges* **5**, 219 (1903).
- [26] E. Persson, *Z. Phys* **57**, 115 (1929).
- [27] R. A. de Groot, F. M. Mueller, P. G. v. Engen, and K. H. J. Buschow, *Phys. Rev. Lett.* **50**, 2024 (1983).
- [28] I. Žutić, J. Fabian, and S. Das Sarma, *Rev. Mod. Phys.* **76**, 323 (2004).
- [29] K. A. Kilian and R. H. Victora, *J. Appl. Phys.* **87**, 7064 (2000).
- [30] E. Y. Tsymbal and D. G. Pettifor, in *Solid. State. Phys.*, Vol. 56 (Elsevier, 2001) pp. 113–237.
- [31] C. J. Palmstrøm, *Prog. Cryst Growth. Charac. Mater.* **62**, 371 (2016).
- [32] H. Wijn, in *Magnetic Properties of Metals* (Springer, 1991) pp. 95–158.
- [33] C. Felser and A. Hirohata, *“Heusler Alloys”* (Springer, 2015).
- [34] P. J. Brown, K. U. Neumann, P. J. Webster, and K. R. A. Ziebeck, *J. Phys: Cond Matt.* **12**, 1827 (2000).
- [35] K. Kobayashi, R. Umetsu, R. Kainuma, K. Ishida, T. Oyamada, A. Fujita, and K. Fukamichi, *Appl. Phys. Lett.* **85**, 4684 (2004).
- [36] T. Graf, C. Felser, and S. S. Parkin, *Prog. Solid. State. Chem.* **39**, 1 (2011).
- [37] J. M. Shaw, E. K. Delczeg-Czirjak, E. R. J. Edwards, Y. Kvashnin, D. Thonig, M. A. W. Schoen, M. Pufall, M. L. Schneider, T. J. Silva, O. Karis, K. P. Rice, O. Eriksson, and H. T. Nembach, *Phys. Rev. B* **97**, 094420 (2018).
- [38] C. Liu, C. K. Mewes, M. Chshiev, T. Mewes, and W. H. Butler, *Appl. Phys. Lett.* **95**, 022509 (2009).
- [39] M. A. Schoen, D. Thonig, M. L. Schneider, T. Silva, H. T. Nembach, O. Eriksson, O. Karis, and J. M. Shaw, *Nat. Phys.* **12**, 839 (2016).
- [40] I. Galanakis, P. H. Dederichs, and N. Papanikolaou, *Phys. Rev. B* **66**, 174429 (2002).
- [41] I. Galanakis and P. Mavropoulos, *J. Phys: Cond. Matter.* **19**, 315213 (2007).
- [42] M. I. Katsnelson, V. Y. Irkhin, L. Chioncel, A. I. Lichtenstein, and R. A. de Groot, *Rev. Mod. Phys.* **80**, 315 (2008).
- [43] H. C. Kandpal, G. H. Fecher, and C. Felser, *J. Phys. D: Appl. Phys.* **40**, 1507 (2007).
- [44] B. Balke, S. Wurmehl, G. H. Fecher, C. Felser, and J. Kübler, *Sci. Tech. Adv. Mater.* **9**, 014102 (2008).
- [45] S. Picozzi, A. Continenza, and A. J. Freeman, *Phys. Rev. B* **69**, 094423 (2004).
- [46] G. M. Müller, J. Walowski, M. Djordjevic, G.-X. Miao, A. Gupta, A. V. Ramos, K. Gehrke,

- V. Moshnyaga, K. Samwer, J. Schmalhorst, *et al.*, *Nat. Mater.* **8**, 56 (2009).
- [47] A. Mann, J. Walowski, M. Münzenberg, S. Maat, M. J. Carey, J. R. Childress, C. Mewes, D. Ebke, V. Drewello, G. Reiss, *et al.*, *Phys. Rev. X.* **2**, 041008 (2012).
- [48] D. Steil, O. Schmitt, R. Fetzner, T. Kubota, H. Naganuma, M. Oogane, Y. Ando, A. Suszka, O. Idigoras, G. Wolf, *et al.*, *New. J. Phys.* **16**, 063068 (2014).
- [49] D. Steil, S. Alebrand, T. Roth, M. Krauß, T. Kubota, M. Oogane, Y. Ando, H. C. Schneider, M. Aeschlimann, and M. Cinchetti, *Phys. Rev. Lett.* **105**, 217202 (2010).
- [50] J.-P. Wüstenberg, D. Steil, S. Alebrand, T. Roth, M. Aeschlimann, and M. Cinchetti, *Phys. Status Solidi B* **248**, 2330 (2011).
- [51] Supplementary Material is available for this article.
- [52] S. Jana, J. A. Terschlüsen, R. Stefanuik, S. Plogmaker, S. Troisi, R. S. Malik, M. Svanqvist, R. Knut, J. Söderström, and O. Karis, *Rev. Sci. Instrum.* **88**, 033113 (2017).
- [53] S. Mizukami, D. Watanabe, M. Oogane, Y. Ando, Y. Miura, M. Shirai, and T. Miyazaki, *J. Appl. Phys.* **105**, 07D306 (2009).
- [54] A. Kumar, F. Pan, S. Husain, S. Akansel, R. Brucas, L. Bergqvist, S. Chaudhary, and P. Svedlindh, *Phys. Rev. B* **96**, 224425 (2017).
- [55] In Ref. [54] the room temperature FMR data does not show the trend we are reporting here. This has later been found to be related to the limited frequency range studied in that work. For this work we have repeated the FMR measurements with a more extended frequency range, and now find the same trends at room temperature as at low temperatures, i.e., Gilbert damping decreases monotonously with increasing growth temperature.
- [56] O. Eriksson, A. Bergman, L. Bergqvist, and J. Hellsvik, *Atomistic Spin Dynamics*, Foundations and Applications (Oxford University Press, 2016).
- [57] U. Atxitia, O. Chubykalo-Fesenko, J. Walowski, A. Mann, and M. Münzenberg, *Phys. Rev. B* **81**, 174401 (2010).